Nanoscale

Emulsion Droplets as A Dynamic Interface for Direct and Large-Scale Synthesis of Ultrathin Free-Standing Mesoporous Silica Films as well as 2D Polymeric and Carbon Nanomaterials

Journal:	*Nanoscale*
Manuscript ID	NR-ART-10-2015-007058.R1
Article Type:	Paper
Date Submitted by the Author:	16-Dec-2015

Complete List of Authors:	Li, Guangtao; Tsinghua University, Chemistry Li, Jian; Tsinghua University, Chemistry Zhu, Wei; Tsinghua University, Department of Chemistry Ji, jingwei; Tsinghua University, Chemistry Wang, Peng; Tsinghua University, Chemistry Wang, Chen; Tsinghua University, Chemistry Yin, Xianpeng; Tsinghua University, Chemistry Wang, Hui; Tsinghua University, Chemistry Lan, Yue; Tsinghua University, Chemistry Gao, Ning; Tsinghua University, Department of Chemistry

Journal Name

ARTICLE

Emulsion Droplets as A Dynamic Interface for Direct and Large-Scale Synthesis of Ultrathin Free-Standing Mesoporous Silica Films as well as 2D Polymeric and Carbon Nanomaterials†

Received 00th January 20xx,
Accepted 00th January 20xx

DOI: 10.1039/x0xx00000x

www.rsc.org/

Jian Li, ‡ Wei Zhu, ‡ Jingwei Ji, Peng Wang, Chen Wang, Xianpeng Yin, Hui Wang, Yue Lan, Ning Gao and Guangtao Li*

Efficient synthesis of free-standing mesostructured two-dimensional (2D) nanofilms with high-yield as well as good control of composite, mesophase structure, orientation of pore channel and thickness represents a big challenge. In this work, it was serendipitously found that microemulsion droplets of tetraethylorthosilicate(TEOS) could serve as a novel dynamic interface for continuous growth of nanofilms. Based on this finding, a general, efficient strategy for direct and large-scale synthesis of free-standing mesoporous silica films (FSMSFs) was developed. Remarkably, with the careful control of the synthesis conditions, the FSMSFs with high-yield as well as good control of composite, mesophase structure, orientation of pore channel and thickness could be efficiently achievable. More importantly, by using polymerizable surfactants the preorganized monomers in nanochannels of the resultant silica films could be further converted into 2D polymer and carbon nanomaterials as well as metal particle-decorated forms, as exemplified by using pyrrole-terminated surfactants, demonstrating a powerful method to creat 2D inorganic, organic or hybrid functional nanomaterials.

Introduction

The rational design and synthesis of two-dimensional (2D) nanostructured materials have drawn considerable attention due to their highly enhanced interface effects and great potential for applications in adsorption, separation, catalysis, sensors, energy conversion and storage, and so on.[1] Among these, ultra-thin free-standing mesoporous silica films (FSMSFs) are both of technological and scientific interest owing to the low dielectric constants, high surface area, good mechanical strength and chemical stability.[2] In the past two decades, it was found that the two-phase interfaces could provide a useful platform for self-assembly process, and correspondingly many strategies could be designed to produce FSMSFs.[2b, 3] A liquid-solid interface was first used by Brinker's group in the preparation of mesoporous silica films on solid substrates through evaporation-induced self-assembly. Inspired by this genial work, many methods including stöber solution growth,[4] evaporation-induced self-assembly process,[2a] electro-assisted approach,[5] and so on have been developed to create FSMSFs by isolating the pre-prepared silica films from the substrate to get free-standing state. However, this strategy often suffers from the hard isolation and break of the film integrity during isolation,[3a] meanwhile, the unsupported growth of FSMSFs at static interfaces (air-water or oil-water interface) has also been introduced to meet the annoying issues.[6] However, the layer-by-layer (LBL) batch-type production shows lower efficiency, and the FSMSFs growth under acidic condition is always labile and thermally unstable.[7] Although the film growth at interfaces under alkaline condition can significantly improve its stability, a large amounts of powder by-products in bulk phase restrict the efficiency, and at the same time the thickness and mesophase structure of the resulting FSMSFs is difficult to be controllable.[8] Recently, increased works have been devoted to use emulsion systems, which possess gigantic biphase interface, for effectively creating mesoporous nanomaterials.[2b,9] Nevertheless, the reported products always show core-shell structure or nanofiber morphology. Thus, although great progress has been made in the past years, the direct and large-scale synthesis of FSMSFs, particularly with a good control of composites, mesophase structure, orientation of pore channel and thickness, is still a big challenge.

In the present study, we report a novel strategy for the facile large-scale synthesis of ultra-thin FSMSFs based on a dynamic emulsion interface growth approach (Scheme 1). We found that, instead of the closed silicate shell structure observed in previous works, under a given condition emulsion droplets of tetraethoxysilane (TEOS) could serve as both silica

Department of Chemistry and Key Lab of Organic Optoelectronics & Molecular Engineering, Tsinghua University, Beijing, 100084, P. R. China.
E-mail: lgt@mail.tsinghua.edu.cn; Tel: +86-010-62792905.
†Electronic Supplementary Information (ESI) available: See DOI: 10.1039/x0xx00000x
‡These authors contributed equally to this work.

source and dynamic interface to produce extended nanofilms. At TEOS-water interface a mesostructured layer is initially

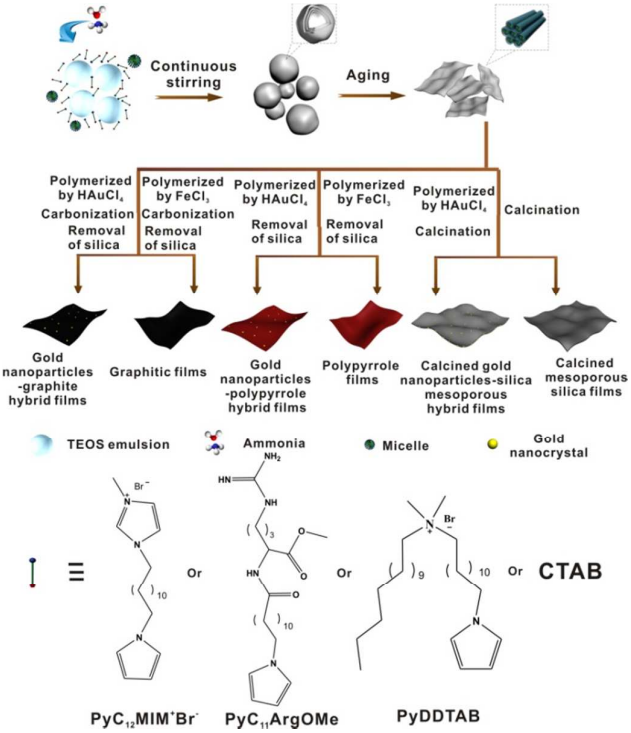

Scheme 1 Schematic illustration of the preparation of ultra-thin FSMSFs via the dynamic emulsion interface growth and their derived polymer/ graphitized / hybrid films.

formed, and probably due to electrostatic interaction with the used structure-directing agents (surfactant) constantly diffusion inward and assemble onto TEOS droplet surface. Consequently, at TEOS-water interface, the cooperative self-assembly of the freshly generated silica oligomer species and surfactants affords continuously FSMSFs in LBL growth fashion. This strategy is characterized with following advantages. Firstly, this dynamic growth method allows for direct, efficient and large-scale synthesis of FSMSFs with high yield (ca. 85%). Secondly, through careful control of ammonia concentration and the type of surfactants, FSMSFs with good control of thickness and mesophase structure are achievable. Thirdly, this approach is generally applicable for different surfactants including commercial cetyltrimethyl ammonium bromide (CTAB) and thus broad its applications. Importantly, by using polymerizable surfactants the preorganized monomers in mesoporous channels of the resultant silica films could be further converted into mesostructured 2D polymer and carbon nanomaterials as well as metal nanoparticles-decorated forms through in-situ polymerization or carbonization, indicative of a powerful method to create inorganic, organic or hybrid 2D functional nanomaterials. To the best of our knowledge, this is the first report on the facile and large-scale synthesis of FSMSFs based on a novel dynamic emulsion interface growth method.

Results and discussion

In a typical synthesis, an ionic liquid-based amphiphile bearing terminal pyrrole moiety 12-(1H-pyrrole-1-yl)-N-dodecyl-3-methyl-imidazolium-bromide (denoted as $PyC_{12}MIM^+Br^-$; Py=pyrrole, MIM=methylimidazolium; see Scheme 1) (0.01 g) was first used as surfactant and dissolved in 10 ml water with 122 µl TEOS. After 10 min of stirring, 30 µl $NH_3{\cdot}H_2O$ (28%) was added dropwise under vigorous stirring, and a molar ratio of 54:3:59 (TEOS/$PyC_{12}MIM^+Br^-$/$NH_3{\cdot}H_2O$) was established. After 6 hours of further stirring in an ice bath, the solution was left standing at 80°C for 12 h in an autoclave. A white powder was collected by centrifugation, washed with water, and dried in air. The yield of FSMSFs prepared by $PyC_{12}MIM^+Br^-$ (denoted as FSMSFs-$PyC_{12}MIM^+Br^-$-0.055, 0.55 is the ratio of surface to TEOS) was ca. 85%. Fig. 1A and 1B shows the scanning electron microscope (SEM) images of the resultant FSMSFs with micrometer scale. The FSMSFs resemble crumpled silk veils (Fig. 1C), which are quite different from the ones obtained by static interface growth method. The film thickness is measured for 30~35 nm (Fig. 1B insert). High-resolution transmission electron microscope (HRTEM, Fig. 1D) reveals a wormlike mesoporous structure throughout the film, which is in agreement with the X-ray diffraction (XRD) pattern that has one broad Bragg diffraction peak located at 2θ=2.4° with d spacing of 3.4 nm (Fig. 3A, blue curve). The surface area of the film is 1017 $m^2\ g^{-1}$, and the pore size is about 2.2 nm (Table S1†). Through this preparation method, large-scale synthesis of ultra-thin FSMSFs is facilely accessible.

In our preparation, the molar ratio of TEOS, surfactant, and $NH_3{\cdot}H_2O$ is of significance in FSMSFs growth and the formed mesostructure. It is found that the ratio of $NH_3{\cdot}H_2O$ and TEOS at 1.1 and surfactant/TEOS ratio in the range of 0.01 to 0.11 is favourable for the growth of FSMSFs. As shown in Scheme S1†, the morphology of the resultant products is strongly dependent on the used preparation conditions. For example, when the ratio of surfactant to TEOS is fixed at 0.055, the increasing of $NH_3{\cdot}H_2O$/ TEOS ratio higher than 1.1 would afford more agglomerated particles accompanied with gradual disappearance of FSMSFs product. Interestingly, when the ratio approaches to 4.1, the morphology would change to be nanotube. In fact, in the literature it had been reported that the high rate of condensation of silica at high alkalinity resulted in hollow mesostructured tubes.[10] Liquid crystal phase transformation from a lamellar to tubular phase was believed to be responsible for the formation of the observed tubular structure. However, for our case we still don't know the exact formation mechanism or driving force for the observed nanotubes. On the contrary, when the ratio reduced less than 1.1, large lumps aggregated by small particles were obtained. Meanwhile, the amount of the surfactant is important to tune the mesostructure of the formed FSMSFs. With the ratio of $NH_3{\cdot}H_2O$ to TEOS at 1.1, the increasing of the ratio of surfactant to TEOS in the range of 0.01 to 0.11 could give more ordered mesostructure of FSMSFs (denoted as FSMSFs-$PyC_{12}MIM^+Br^-$-0.11 Fig. S1†). As shown in Fig. 1E, majority of hexagonal packing of perpendicular channels as well as small amount of domain comprising channels aligned parallel to the

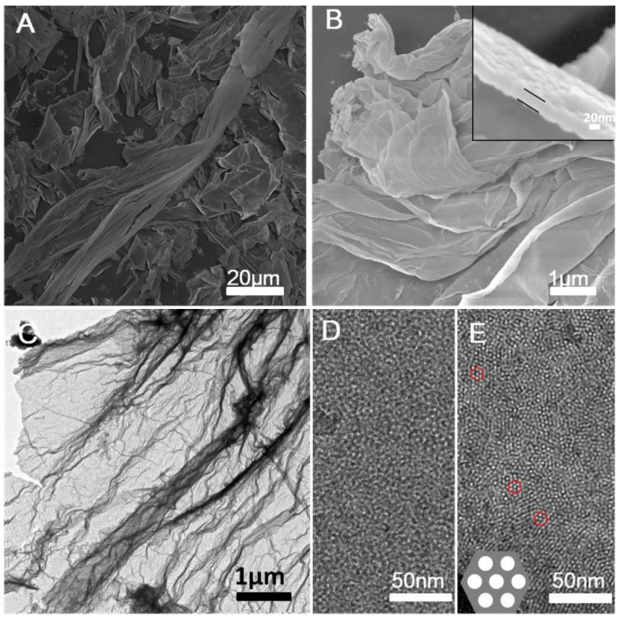

Fig. 1 A-B) SEM and C-D) TEM images of the resultant $PyC_{12}MIM^{+}Br^{-}$-FSMSFs with wormlike mesoporous structure at different magnifications. (Inset: cross-section SEM image); E) TEM image of the $PyC_{12}MIM^{+}Br^{-}$-FSMSFs with hexagonal packing of perpendicular channels.

surface appeared in the film. By using 2D grazing incidence small-angle X-ray scattering (GISAXS), we tried to provide further evidence for the formation of hexagonal packing of perpendicular channel structure over the film. However, due to the difficulty of achieving the deposition of flat film of the prepared free-standing silica films onto a solid substrate, the performed experiments failed. Nevertheless, the top-view TEM images (Fig. 1E and Fig. S1B in Supporting Information) revealed that the most of channels are perpendicular to the silica film, but a small amount of domain is comprised of channels aligned parallel to the surface. From the tilted edge (Fig. S1C), it can be observed that majority of mesoporous channels were nearly continuous throughout a cross-section of the film along the vertical direction of the silica film. In fact, similar results have also been reported in literature.[4] Additionally, the XRD pattern (Fig. 3A) of the silica film showed a strong diffraction peak as well as two weak diffraction peaks, associated with the 10, 11, and 20 reflections of hexagonal symmetry with the space group p6mm, indicative of the formation of ordered mesochannel structure. At present we cannot provide an explicit mechanism for the formation of hexagonal packing of perpendicular channels. A possible mechanism may be similar to that proposed Zhao's work.[4] Namely, the cylindrical surfactant micelles that are perpendicularly orientated on the droplet surface formed, and then after solution assembly and growth, mesoporous silica films with perpendicular channels are obtained. However, when the ratio of $NH_3 \cdot H_2O$ to TEOS was further increased higher than 0.11, the reaction rate became faster, and finally the morphology was changed to spheres.

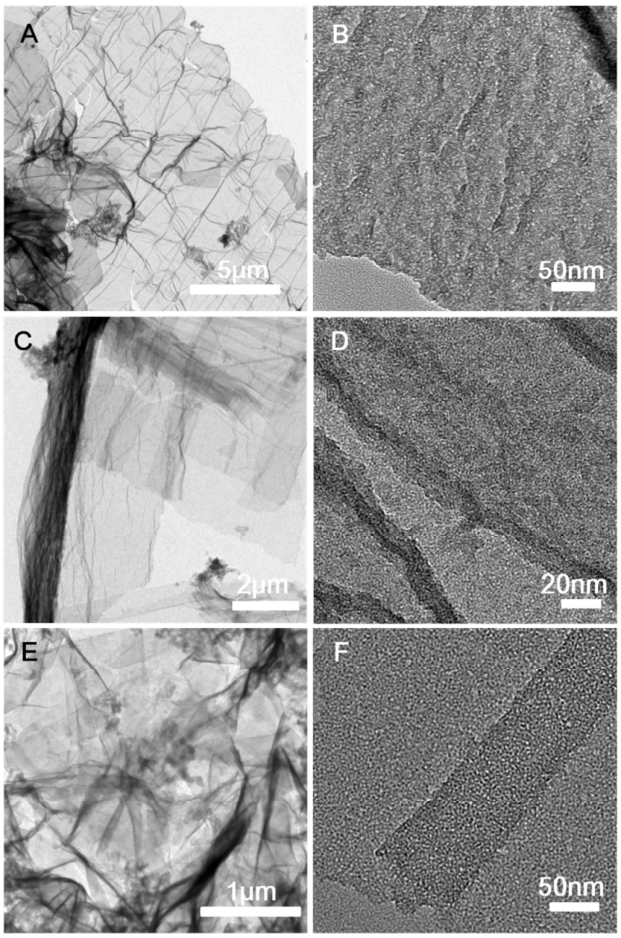

Fig. 2 TEM images and the corresponding HRTEM images of A-B) the resultant FSMSFs prepared by using PyC_{11}ArgOMe, C-D) PyDDTAB , and E-F) CTAB as surfactant, respectively.

The developed strategy is generally applicable for producing FSMSFs by using different surfactants. Besides $PyC_{12}MIM^{+}Br^{-}$, three other surfactants (L)-2-(12-(1H-pyrrole-1-yl) dodecamide)-4-Guanidine-Methyl butyrater (denoted as PyC_{11}ArgOMe), N,N-dimethyl-N-[12-(1H-pyrrole-1-yl) dodecyl] tetradecyl ammonium bromide (denoted as PyDDTAB), and CTAB (Scheme 1) were also used in our work for demonstration. The synthetic procedure was similar but with different surfactant and ammonia amount. In Fig. 2A and Fig. S2C†, large silk-like FSMSFs with thickness of 20-24 nm were clearly observed for the case of PyC_{11}ArgOMe. HRTEM image (Fig. 2B) and XRD pattern (Fig. 3A, red curve) revealed the wormlike mesostructure. N_2 sorption isotherm showed a curve with the characteristics of type II and IV as well as a distinct hysteresis loop of H3 (Fig. 3B), which was caused by folding of the thin films. The surface area was measured as 220.6 $m^2\ g^{-1}$, and pore size as 2.7 nm (Fig. 3C). Compared with the case of $PyC_{12}MIM^{+}Br^{-}$, PyC_{11}ArgOMe exhibits excellent capability of creating FSMSFs with a yield more than 90%. In addition, by adjusting the amount of surfactant and ammonia, a thicker FSMSF with a thickness of 95 nm is accessible (Fig. S2†- S3†).

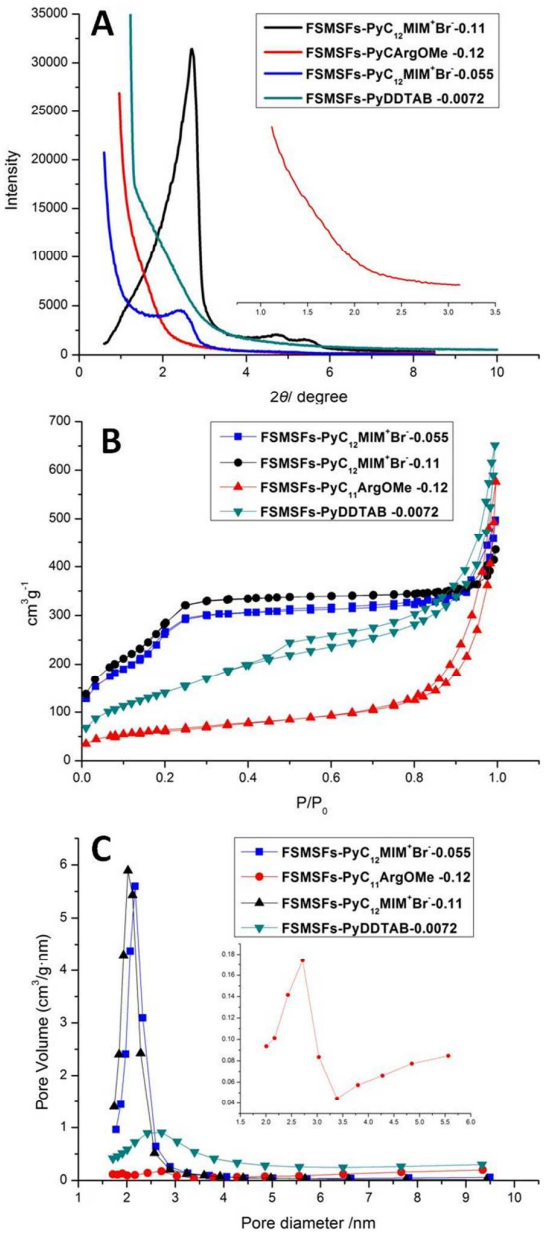

Fig. 3 A) X-ray diffraction patterns, B) N_2 adsorption-desorption isothermals and C) Pore-size distributions of FSMSFs-$PyC_{12}MIM^+Br^-$, FSMSFs-PyC_{11}ArgOMe and FSMSFs-PyDDTAB. The result of PyC_{11}ArgOMe -FSMSFs in the degree region between 1.2 and 3.2 is given as inset in A and the result of PyC_{11}ArgOMe-FSMSFs in the pore diameter region between 2 nm and 6 nm is given as inset in C.

For the case of PyDDTAB, we also got the similar FSMSFs with thickness of 40-65 nm (Fig. 2C-D and Fig. S2A†). Importantly, for commercial surfactant CTAB, SEM and TEM images also showed the successful preparation of FSMSFs with thickness of 30 nm (Fig. 2E-F and S2B†). It should be noted that, probably due to the different emulsifying properties of the surfactants, the yield of the formed FSMSFs is also different (Table S2†).

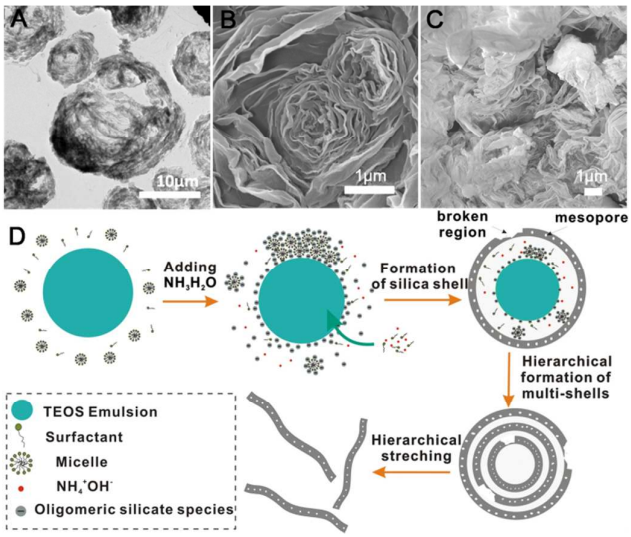

Fig. 4 A) TEM image of loose silica cages formed after reacting for 0.5 h; SEM images of B) cabbage-like mesoporous silica composites formed after reacting for 3 h and C) stretched silica films stripped from (B) after stirring for another 3 h; D) the proposed formation mechanism for the FSMSFs.

Nevertheless, these results clearly suggested that our method is a general approach for synthesis of FSMSFs.

Compared with the soft-templating method at static interfaces, the synthesis of FSMSFs via dynamic approach described in this work is still unknown. To facilitate a deep understanding of the formation mechanism, the morphological and structural evolution of the product of $PyC_{12}MIM^+Br^-$-based system with reaction time was systematically investigated. At the beginning, under stirring a milky emulsion containing TEOS and surfactant was formed. The emulsion appearance maintained even after the addition of ammonia for 20 min. After that, the solution start to become turbid accompanied with the disappearance of the droplets. At this time, the loose cage-like hollow spheres with folded thin shell and diameter of 3~10 μm were observed (Fig. 4A), indicative of a thin silica shell coated on the outside of TEOS emulsion. With the further stirring, the solution became more turbid. After the reaction for 3 h, a small amount of products were taken out to show a cabbage-like structure formed by the stacking of multilayer mesoporous silica shells (Fig. 4B). With the continue stirring for another 3 h, the mesoporous silica films were stripped from the cabbage-like microspheres from the outer layer to inner layer (Fig. 4C), indicating a LBL stripping process. These films could be stretched to relative planar film by further aging process. Note that the thickness of the films was almost the same during the aging period, indicating that the majority of TEOS was depleted in the former process. Controlled experiments under static but identical reaction conditions at room temperature or 80°C yielded the irregular silica microspheres with a diameter of ca. 1μm (Fig. S4A†-S4B†) and rigid platelets with thickness more than 0.5 μm (Fig. S4C†-S4D†), which ruled out the air-water interface growth

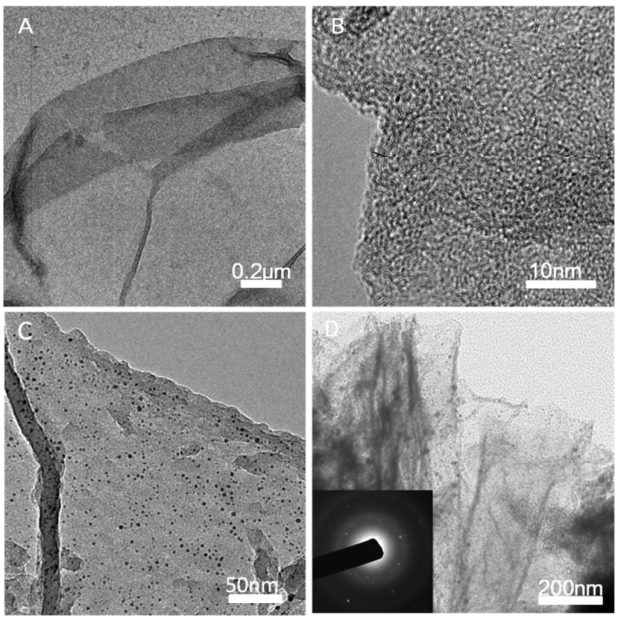

Fig. 5 A) TEM image of the PPyF; B) HRTEM image of the GF; C) TEM images of the Au NPs-decorated FSMSFs and D) Au-GFs(insert: electron diffraction pattern).

mechanism. Also, FSMSFs could be prepared by using Teflon bottles (Fig. S4E†-S4F†), which eliminated the glass substrate growth as the precious report.[4]

Based on the above results, we proposed an in LBL growth mechanism on the dynamic emulsion interface (Fig. 4D). In the initial stage, owing to the immiscibility of TEOS in water, TEOS emulsion deroplets with relative stable morphology were formed in the surfactant-containing solution. With the addition of a little ammonia, hydrolysis of TEOS yielded the low negative-charged oligomeric silicate species, which were relative hydrophobic and tended to accumulate on the outside surface of TEOS droplets. Accompanied with a cooperative self-assembly of the silicate species with positive-charged micelles formed by surfactant, a mesoporous intermediate is first generated at the TEOS-water interface. With continuous generation of oligomeric silicates on TEOS surface under the presence of ammonia, the surfactant molecules were induced toward TEOS-water interface through electrostatic interaction and a new mesoporous silica layer again formed. Under stirring the constant consumption of TEOS and correspondingly growth of mesostructured layers at the interface inevitably lead to the formation of free-flowing cabbage-like composite composed of mesostructured silica thin layers. With prolonged aging, these composites could be stretched into silk-like free-standing films. Based on this mechanism, the effect of ammonia on the formation of FSMSFs could be explained. The higher ammonia concentration leads to an increased hydrolysis and condensation of TEOS, easily breaking the TEOS emulsion. In contrast, at lower ammonia concentration, the slow hydrolysis process failed to form a negative charged silicate layer to coat on the TEOS droplets. With the continuous stirring, more free oligomeric silicates tended to detach from the droplet surface into the solution, leading to the formation of small silica particles.

In our work, we performed the measurement on the process of surface zeta-potential changes with the expectation of further confirming the LBL growth mechanism proposed. However, we didn't obtain rational results. In the case of the conventional LBL approach, it is very easy to obtain the intermediates (layers) with different charges and thus to allow for monitoring the surface zeta-potential changes during the LBL growth. However, in our case the growth of the silica films proceeds fast and continually, and thus it is quite difficult to trap the intermediates for the measurement of the surface zeta-potential changes. Therefore, it is difficult to measure the process of surface zeta-potential changes to further confirm the LBL growth mechanism induced by electrostatic interactions.

During the formation of FSMSFs, the used surfactants are densely packed within the formed mesochannels in a controlled fashion. It can be conceivable if the surfactant is polymerizable amphiphile, the monomer moieties are also preorganized in the mesoporous channels. Clearly, our strategy not only provides a direct way to produce FSMSFs, but also offers good possibilities to achieve the generation of other mesostructured 2D materials in through in-situ polymerization and carbonization of monomers in the confined nanochannels.[11] As a proof of our concept, the prepared $PyC_{12}MIM^{+}Br^{-}$-FSMSFs-0.055 composites were exposed to a $CHCl_3$ solution of $FeCl_3$ (oxidant). After 24 h reaction followed by the removal of silica template, we indeed found that the packed surfactants (ie. monomer) in the mesochannels were converted into polypyrrole films with a mesoporous structure. Fig. 5A shows the typical TEM image of the polypyrrole film (denoted as PPyF) with smooth surface. The porous structure descending from the templates is also clearly observed (Fig. S6A†). As expected, after the polymerization followed by carbonization in nitrogen flow at 800°C, the graphitized film (denoted as GFs), which was formed by ultrathin carbon wires based on the strong π-π interaction, is also facilely accessible after the removal of silicate template. In Fig. 5B, a weak ordered turbostratic carbon structure and small crystalline domains with d spacing of 0.36 nm are clearly observable. The Raman spectrum (Fig. S7C†) shows two peaks at 1324 (D band) and 1594 cm^{-1} (G band).The intensity ratio of the G and D bands (I_G/I_D) is 0.35.

Besides $FeCl_3$, many metal salts possess enough oxidative potentials to induce polymerization of monomer units like pyrrole, meanwhile they self are reduced into metal nanocrystals.[12] This redox behaviour suggests that our strategy could be further extended to synthesize a series of metal nanoparticle-decorated polymer or carbon nanofilms. As a demonstration, in our case, tetrachloroauric acid was selected as oxidant to polymerize the pyrrole moiety of $PyC_{12}MIM^{+}Br^{-}$

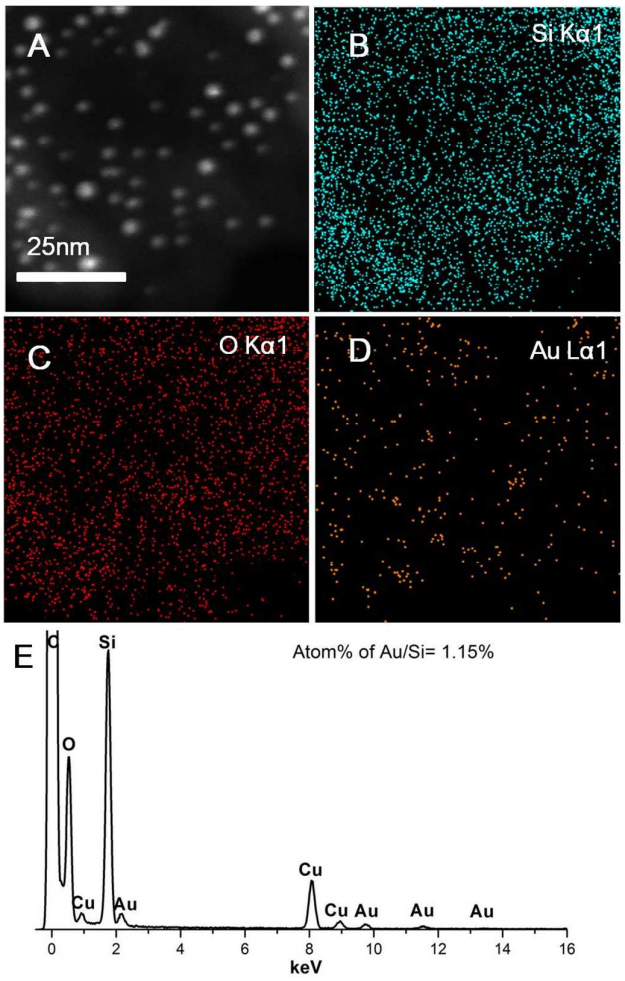

Fig. 6 A) STEM image of a corner of Au nanoparticles-decorated FSMSFs; B-D) the corresponding STEM element mapping of Si, O, and Au elements; E) element content in this area.

surfactant in the resultant silica films. As expected, the ultrasmall gold nanoparticles (NPs) were grown confined within the mesochannels with the simultaneous formation of polypyrrole. As shown in Fig. 5C and Fig. S5, numerous Au NPs with the size of 2.0-3.0 nm were distributed within the mesoporous channels. The scanning transmission electron microscopy (STEM) mapping (Figure 6A-D) further confirmed the presence of all the expected elements, including gold, silicon and oxygen elements. And the atom ratio of Au to Si was measured to be 1.15%. From the UV/Vis spectrum in Fig.S7A†, besides the broad absorption band of polypyrrole at 400 nm, the typical absorption of Au NPs at 510 nm was also detected in the gold nanoparticles decorated polypyrrole film (denoted as Au-PPyFs) sample. Correspondingly, the additional carbonization treatment afforded the Au NPs decorated graphitic films (denoted as Au-GFs Fig. 5D). The most of Au nanoparticles with size of 2~3 nm were mingled into the weak-ordered graphited layers. Selected-area electron diffraction confirmed the high crystallinity of the gold NPs. By using the Au-GFs for catalysing the reduction of nitrophenol, the almost 100% conversion for three cycles (Fig. S8†) demonstrated a highly catalytic activity. This good catalytic activity can be attributed to the microporous carbonaceous shell to promote the mass diffusion, high crystallinity of gold NPs to improve the catalytic efficiency, as well as the ultrathin carbon films to prevent the NPs aggregation. Thus, through the rational combination of oxidative agents and the FSMSF structure, the reported strategy provides us tremendous opportunities for the design of novel 2D functional nanomaterials.

Experiments

Synthetic procedures

Synthesis of $PyC_{12}MIM^+Br^-$-FSMSFs: $PyC_{12}MIM^+Br^-$ (10~20 mg) were dissolved in deionized water (10 ml) with vigorous stirring. Then TEOS (122 μL) were added to the solution. After stirring for 10 min, the aqueous ammonia (28 wt%, 30 μL) was added dropwise in the solution. And the resulting solution was stirring in an ice bath for 6 h. Then the mixture was transferred into autoclave, and heated in 80℃ for 12 h. The resulting mixture was passed through the membrane with a pore diameter of 3 μm. The residues on the membrane were washed with water by centrifugation (8000 rpm) and dispersion with three times. The precipitates were dried in air to afford a white powder. The yields were calculated by mass ratio of FSMSFs to total products for at least three times. With the increasing of surfactant amount, the yields decreased slightly.

Synthesis of PyC_{11}ArgOMe-FSMSFs: PyC_{11}ArgOMe (19.2 mg) was dissolved in deionized water (20 ml) with vigorous stirring. Then TEOS (122 μL) and aqueous ammonia (28 wt%, 20 μL) were added to the solution sequentially and the resulting solution was stirring in an ice bath for 12 h. The resulting mixture was light gray and was washed with water by centrifugation and dispersion with three times. Then the resulting mixture was left standing at 80 for 12 h in an autoclave. A white powder was collected by repeating centrifugation, washed with Millipore water, and dried in air.

Synthesis of PPyFs: Anhydrous ferric chloride (0.02 g) was dispersed in chloroform (3 mL) by vigorous stirring. Then $PyC_{12}MIM^+Br^-$-FSMSFs-0.055 (0.01 g) was added subsequently and stirring for 12 h. The resulting yellow solution was washed with water by centrifugation and dispersion for four times to guarantee removing up the iron ions. The as-polymerized $PyC_{12}MIM^+Br^-$FSMSFs-0.055 were spread on the copper grid and etched with HF vapor to obtain the polymer films.

Synthesis of Au-FSMSFs/PPyFs: For the synthesis of Au NPs-decorated $PyC_{12}MIM^+Br^-$-FSMSFs, 0.02 g original $PyC_{12}MIM^+Br^-$FSMSFs-0.055 powder was added into 7 ml H_2O. Then 100 μL 0.2 mol/L $HAuCl_4$ aqueous solution was added to the mixture. After stirring for 6 h, the resulted products were washed by deionized water for 3 times and dried in air to finally form the Au-$PyC_{12}MIM^+Br^-$-FSMSFs. For the synthesis of Au-PPyFs, the Au NPs-decorated $PyC_{12}MIM^+Br^-$-FSMSFs were treated by HF vapor to remove the silica.

Synthesis of GFs or Au-GFs: The as-polymerized $PyC_{12}MIM^{+}Br^{-}$-FSMSFs or Au NPs-decorated $PyC_{12}MIM^{+}Br^{-}$-FSMSFs were carbonized under a nitrogen flow at 800℃ for 3 h. After the removal of silica framework by 5% aqueous HF, the residues were dialyzed thoroughly with deionized water for 1 day.

Catalytic ability and stability of Au-GFs: Catalysis experiments were followed by the previous report.[13] First, 4-nitrophenol (3 mL, 1×10^{-4} M) was mixed with aqueous solution of $NaBH_4$ (0.1 mL, 3×10^{-1} M). Then the Au-GFs (10 mg) were added into the above solution with constant magnetic stirring. UV/Vis absorption spectra were recorded to exam the extent of reaction after filtering catalysts. After each use, the Au-GFs were recycled by simple centrifugation, followed by washing with distilled water and drying in air for the next cycle of catalysis. The catalytic results at different time were carried out by the parallel tests.

Conclusions

In summary, we found that microemulsion droplets of TEOS could serve as a novel dynamic interface for continuous growth of nanofilms. Based on this finding, a general, efficient strategy for direct and large-scale synthesis of ultra-thin FSMSFs was developed. Remarkably, with the careful control of the synthesis conditions, the FSMSFs with high-yield as well as good control of their composite, mesophase structure, orientation of pore channel and thickness could be efficiently achievable. More importantly, in combination with the use of polymerizable surfactant, this strategy can further allow for the preparation of 2D organic, inorganic or metal nanoparticle-decorated hybrid nanomaterials through in-situ polymerization or carbonization of the preorganized monomers in channels of the resultant silicas. Although pyrrole-terminated surfactants are used for the present study, the results are expected to be universal for other types of polymerizable units. Thus, we believe our findings may open up a new route with great extendibility to obtain novel classes of two-dimensional inorganic, organic or hybrid nanomaterials.

Acknowledgements

We gratefully acknowledge the financial support from National Science Foundation of China (No.20141300592, 21121004, and 20141311257), MOST Program (2013CB834502 and 2011CB808403) and Transregional Project (TRR61).

Notes and references

1 (a)M. Xu, T. Liang, M. Shi and H. Chen, *Chem. Rev.*, 2013, **113**, 3766-3798; (b) M. Si, D. Feng, L. Qiu, D. Jia, A. A. Elzatahry, G. Zheng and D. Zhao, *J. Mater. Chem. A*, 2013, **1**, 13490-13495; (c)J. Sakamoto, J. van Heijst, O. Lukin and A. D. Schlueter, *Angew. Chem. Int. Ed.*, 2009, **48,** 1030-1069; (d) F. Wang and X. Wang, *Nanoscale*, 2014, **6**, 6398-6414; (e) G. Yang, C. Zhu, D. Du, J. Zhu and Y. Lin, *Nanoscale*, 2015, **7**, 14217-14231; (f)Y. Fang, Y. Lv, J. Tang, H. Wu, D. Jia, D. Feng, B. Kong, Y. Wang, A. A. Elzatahry, D. Al-Dahyan, Q. Zhang, G. Zheng, D. Zhao, *Angew. Chem. Int. Ed.*, 2015, **54**, 8425-8429.

2 (a)K. Yu, B. Smarsly and C. J. Brinker, *Adv. Funct. Mater.*, 2003, **13,** 47-52;(b) W. Li, Q. Yue, Y. Deng and D. Zhao, *Adv. Mater.*, 2013, **25,** 5129-5152; (c) M. Xu, D. Feng, R. Dai, H. Wu, D. Zhao and G. Zheng, *Nanoscale*, 2011, **3**, 3329-3333.

3 (a) H. Yang, N. Coombs, I. Sokolov and G. A. Ozin, *Nature*, 1996, **381**, 589-592; (b) S. Schacht, Q. Huo, I. G. Voigt-Martin, G. D. Stucky and F. Schueth, *Science*, 1996, **273**, 768-771; (c) Y. Lu, R. Ganguli, C. A. Drewien, M. T. Anderson, C. J. Brinker, W. Gong, Y. Guo, H. Soyez, B. Dunn, M. H. Huang and J. I. Zink, *Nature*, 1997, **389**, 364-368; (d) K.C. Kao, C. H. Lin, T. Y. Chen, Y. H. Liu and C. Y. Mou, *J. Am. Chem. Soc.*, 2015, **137**, 3779-3782.

4 Z. Teng, G. Zheng, Y. Dou, W. Li, C. Y. Mou, X. Zhang, A. M. Asiri and D. Zhao, *Angew. Chem. Int. Ed.* 2012, **51**, 2173-2177.

5 (a) A. Walcarius, E. Sibottier, M. Etienne and J. Ghanbaja, *Nature. Mater.*, 2007, **6**, 602-608; (b) Y. Guillemin, J. Ghanbaja, E. Aubert, M. Etienne and A. Walcarius, *Chem. Mater.*, 2014, **26**, 1848-1858.

6 D. Zhao, Y. Wan and W. Zhou, in Ordered Mesoporous Materials, Wiley-VCH Verlag GmbH & Co. KGaA, Weinheim, 2013, pp.254-260.

7 (a) R. Vogel, C. Dobe, A. Whittaker, G. Edwards, J. D. Riches, M. Harvey, M. Trau and P. Meredith, *Langmuir*, 2004, **20**, 2908-2914; (b) D. Khushalani, A. Kuperman, G. A. Ozin, K. Tanaka, J. Garces, M. M. Olken and N. Coombs, *Adv. Mater.*, 1995, **7**, 842-846.

8 (a) S. S. Park and C.-S. Ha, *Chem. Mater.*, 2005, **17**, 3519-3523; (b) B.Yang and K. J. Edler, *Chem. Mater.*, 2009, **21**, 1221-1231.

9 Y. Li and J. Shi, *Adv. Mater.*, 2014, **26**, 3176-3205.

10 H. P. Lin and C. Y. Mou, *Science*, 1996*,* **273**, 765-768.

11 C. Lin, W. Zhu, H. Yang, Q. An, C. Tao, W. Li, J. Cui, Z. Li and G. Li, *Angew. Chem. Int. Ed.*, 2011, **50**, 4947-4951.

12 (a) S. T. Selvan, J. P. Spatz, H. Klok and M. Möller, *Adv. Mater.,* 1998, **10**, 132-134; (b) A. Chen, H. Wang and X. Li, *Chem. Commun.,* 2005, 1863-1864; (c) S. Fujii, S. Matsuzawa, H. Hamasaki, Y. Nakamura, A. Bouleghlimat and N. J. Buurma, *Langmuir*, 2012, **28**, 2436-2447.

13 R. Liu, S. M. Mahurin, C. Li, R. R. Unocic, J. C. Idrobo, H. Gao, S. J. Pennycook and S. Dai, *Angew. Chem. Int. Ed.*, 2011, **50**, 6799-6802.